SUPPLEMENTARY FIGURES

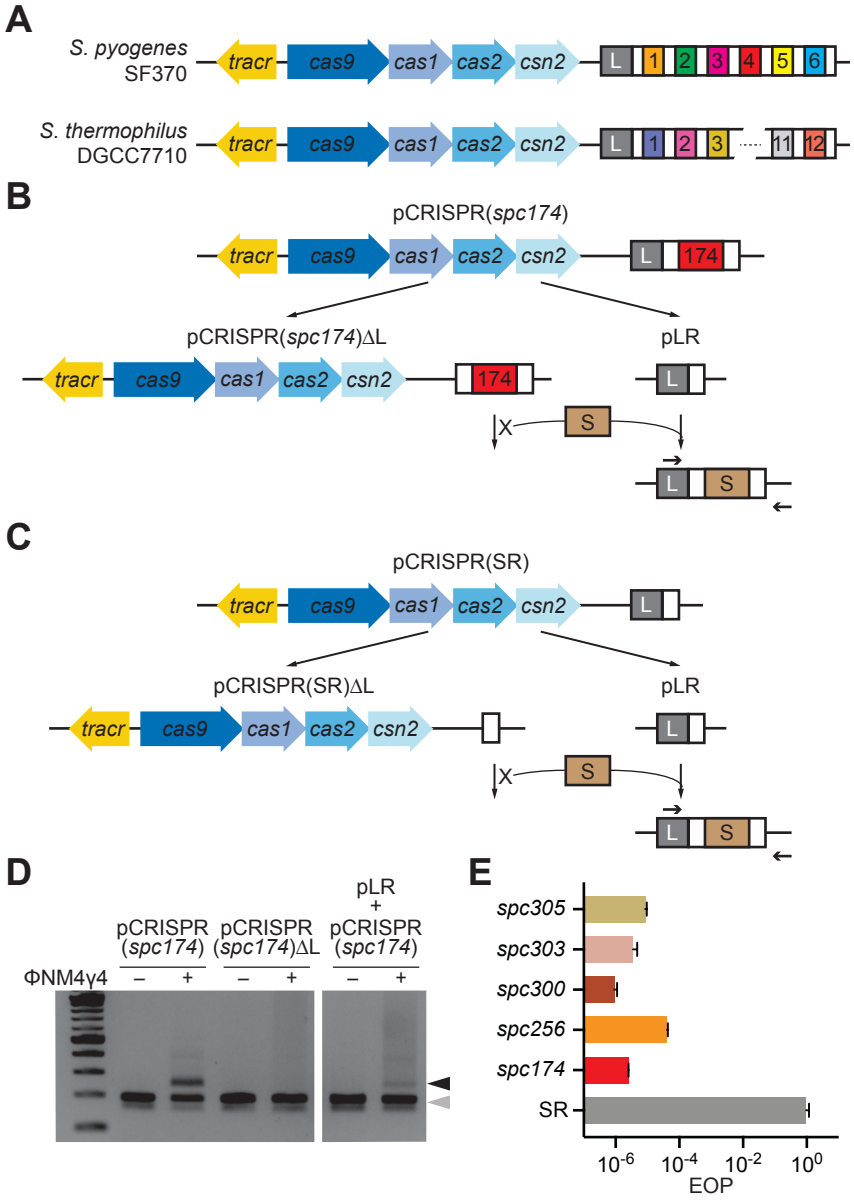

Figure S1. Nussenzweig *et al*.

Figure S1. Design of a two-plasmid system for the study of the effect of pre-existing spacers in type II-A CRISPR-Cas spacer acquisition. Related to Fig. 1. (**A**) Type II-A CRISPR-*cas* loci of *S. pyogenes* SF370 and of *S. thermophilus* DGCC7710. White rectangles, CRISPR repeats; colored and numbered rectangles, spacers; "L", leader sequence; blue arrows, protein-coding genes; yellow arrow, tracrRNA gene. (**B**) pCRISPR(*spc174*) was generated by cloning the *S. pyogenes* SF370 type II-A CRISPR-*cas* locus into the staphylococcal pC194 vector, and the 6-spacer CRISPR array replaced with a single-spacer array harboring the *spc174* sequence. pCRISPR(*spc174*)ΔL was generated after the deletion of the leader, which prevents spacer acquisition *in cis*. To enable the capture of new spacers, a second plasmid

(pE194) containing only the leader and a single repeat was added. Arrows indicate priming sites of oligonucleotides used to detect spacer acquisition via PCR. (**C**) To generate a “no pre-existing spacer” control, pCRISPR(SR)ΔL was constructed, which contains only a single repeat sequence. (**D**) Detection of spacer acquisition by agarose gel electrophoresis of PCR products obtained with primers and plasmid templates shown in (**B**) and (**C**). Grey and black arrows: non-expanded and expanded, respectively, CRISPR arrays. (**E**) Comparison of the efficiency of plaquing (EOP) of ΦNM4γ4 on staphylococci carrying pCRISPR plasmids programmed with spacers *174*, *256*, *300*, *303* and *305*, or without a spacer (SR). Mean ± StDev values of three independent experiments are shown.

A

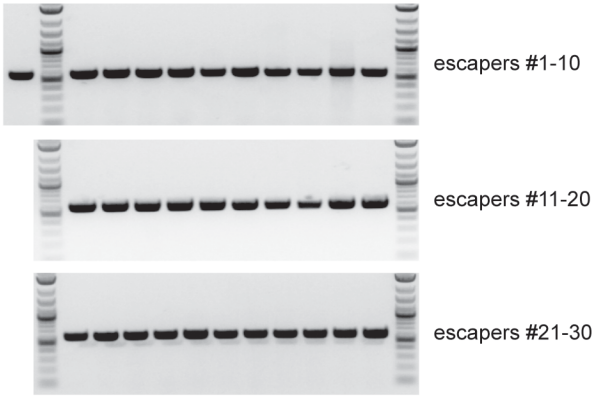

B

frequency	174 protospacer-PAM sequence (5'-3')	mutation
0/30	TGATACATTAACATTTAGTAAATCATTACG-AGG	none
11/30	TGATACATTAACATTTAGTAAATCATTACG-AGA	PAM
06/30	TGATACATTAACATTTAGTAAATCATTACG-AGT	PAM
09/30	TGATACATTAACATTTAGTAAATCATTACG-ATG	PAM
01/30	ACTATGTAATTGTAAATCATTTAGTAATGC-AAG	PAM
02/30	TGATACATTAACATTTAGTAAATCATTGCG-AGG	seed
01/30	ACTATGTAATTGTAAATCATTTAGGAATGC-AGG	seed

Figure S2. Analysis of phages that evade *spc174*-mediated CRISPR immunity. Related to Fig. 2. (**A**) Agarose gel electrophoresis of PCR products obtained after amplification of the *tgt174* region of 30 different ΦNM4γ4 "escapers". (**B**) Summary of the *tgt174* sequences within the PCR products shown in (**A**), with the mutations in the PAM or seed sequences highlighted.

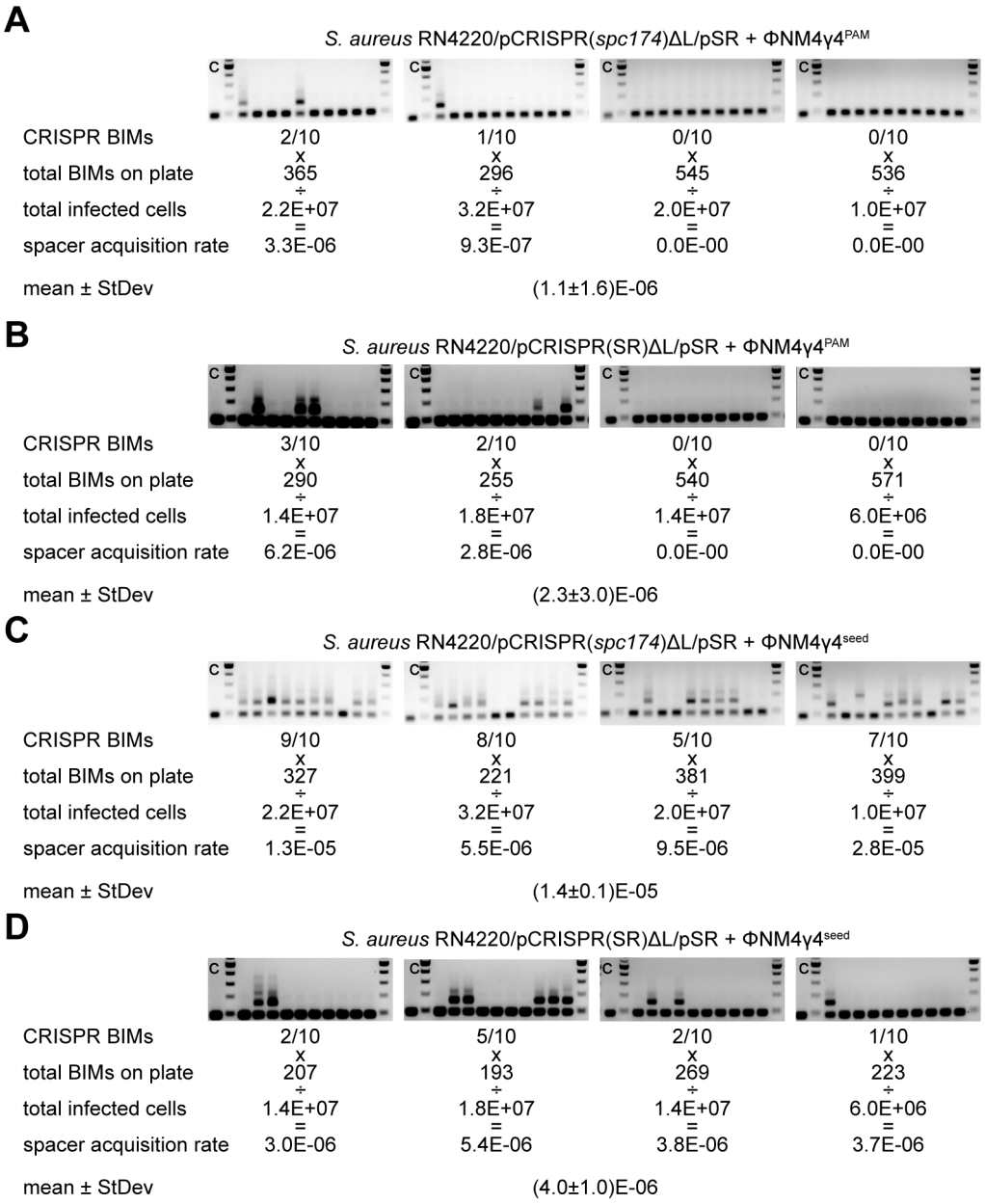

Figure S3. Analysis of spacer acquisition in bacteriophage-insensitive mutant (BIM) colonies. Related to Fig. 2. *S. aureus* RN4220 harboring different CRISPR plasmids were infected with different variants of ΦNM4γ4 phage, mixed with soft agar on plates and incubated for 24 hours to isolate BIM colonies. Four independent experiments were performed for each host/phage combination. The total number of BIM colonies were counted in each plate and ten were selected to detect the acquisition of new spacers by PCR. The results of the agarose gel electrophoresis are shown. “c” indicates a lane where a PCR product corresponding to the CRISPR array uninfected cells was loaded as a negative control. The lane immediately to the right of the control lane contains molecular markers. The PCR results were used to calculate the fraction of BIM colonies that survived through the acquisition of a new spacer (CRISPR BIMs). This fraction was multiplied by the total number of BIM colonies per plate and divided by

the total number of cells infected in the experiment to obtain the spacer acquisition rate. Finally, the values obtained in each experiment where used to calculate the mean and standard deviation of the spacer acquisition rate for each host/phage combination: (**A**) pCRISPR(*spc174*)ΔL/pSR + ΦNM4γ4^{PAM} , (**B**) pCRISPR(SR)ΔL/pSR + ΦNM4γ4^{PAM} , (**C**) pCRISPR(*spc174*)ΔL/pSR + ΦNM4γ4^{seed} , (**D**) pCRISPR(SR)ΔL/pSR + ΦNM4γ4^{seed}.

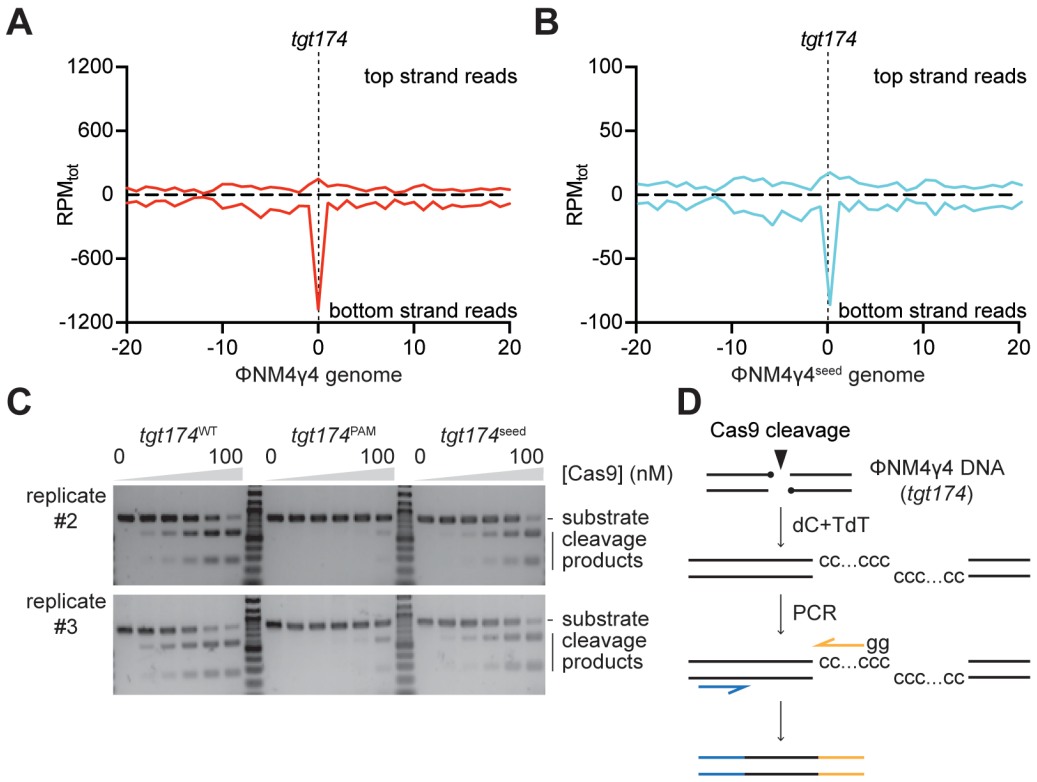

Figure S4. Strand bias of *spc174*-mediated spacer acquisition. Related to Figs. 3 and 4. (**A**) Abundance of the spacer sequences acquired after infection of staphylococci carrying pCRISPR(*spc174*) with ΦNM4γ4, measured as spacer reads per million of total reads (RPM_{tot}), mapped to 1 kb bins of either the top or bottom strands of the phage genome (shown in linear form, with *tgt174* in the center). Average curve of three independent experiments is shown. (**B**) Same as (**A**) but after infection with $ΦNM4γ4^{seed}$. (**C**) *In vitro* cleavage assay of a dsDNA oligonucleotide containing the different *tgt174* sequences shown in Fig. 2A, incubated with increasing concentrations of a 1:1:1 mix of Cas9:tracrRNA:$crRNA^{174}$: 0, 6.25, 12.5, 25, 50 and 100 nM. Substrates and cleavage products were separated by agarose gel electrophoresis. The second and third replicates used for the quantification of Cas9 cleavage shown in Fig. 4B are shown. (**D**) Detection of Cas9 cleavage of the phage genome *in vivo*. Total DNA was extracted 20 minutes after infection and treated with terminal deoxynucleotidyl transferase (TdT) and deoxycytosine (dC) to add poly-dC extensions to the 3' ends of DNA breaks (black dots). The modified DNA was used as template for amplification with a polyG primer (orange arrow) and a second specific primer annealing upstream of the *spc174* target sequence (blue arrow) to detect Cas9 cleavage sites on the phage genome as a PCR product.

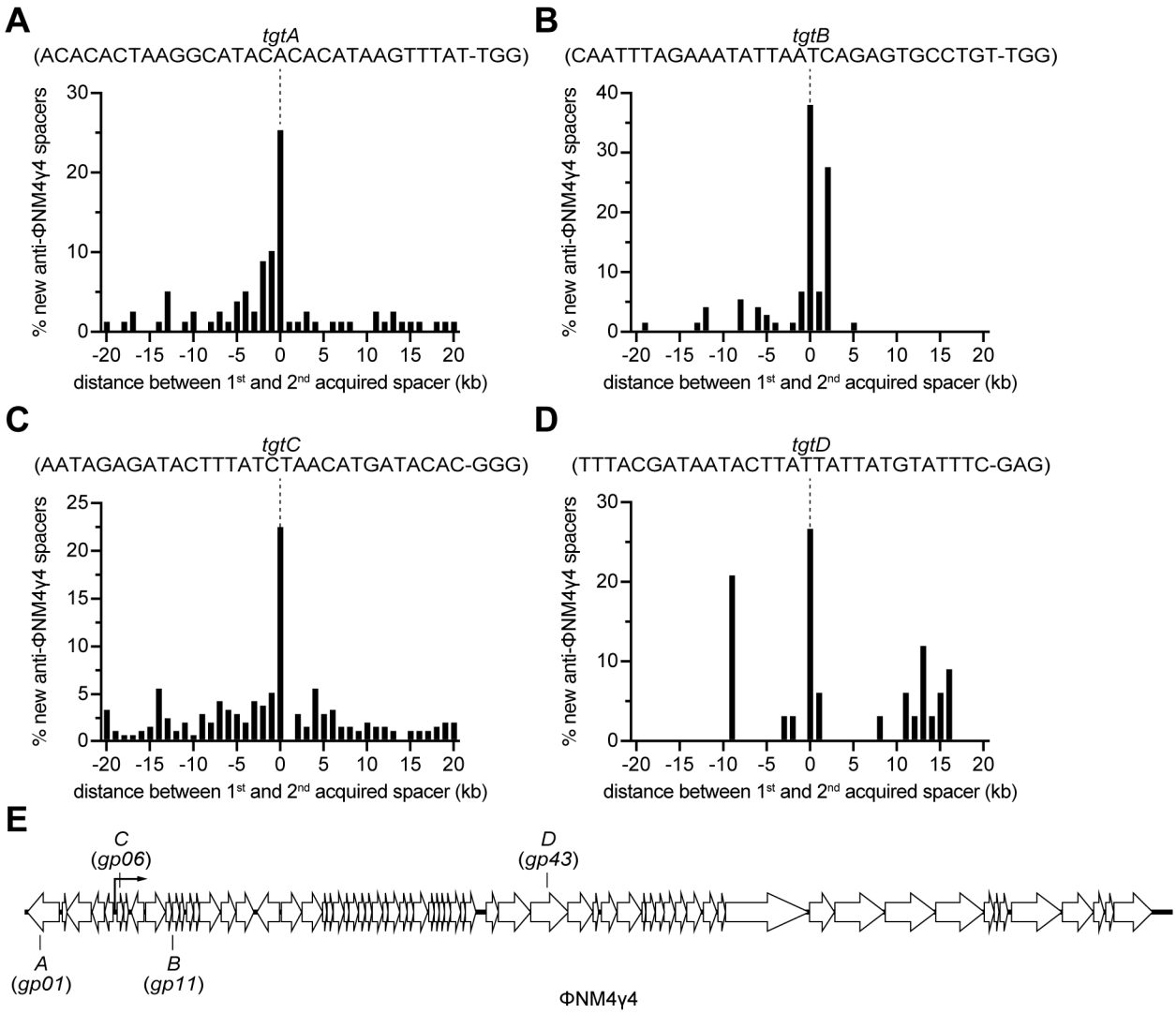

Figure S5. Distance between the targets in the ΦNM4γ4 genome specified by the first and second spacers acquired. Related to Fig. 6. Naïve staphylococci carrying the type II-A CRISPR-Cas system of *S. pyogenes* were infected with ΦNM4γ4. The number of different spacers within 1-kb bins of the ΦNM4γ4 genome are shown. (**A**-**D**) Distribution of distances between the targets specified by the second spacers integrated after the acquisition of the spacers A, B, C and D, respectively; the target sequence specified by the first spacer acquired, which is given a 0 kb position, is shown. (**E**) Location within the ΦNM4γ4 genome of the targets specified by the four first spacers analyzed in (**A**-**D**).

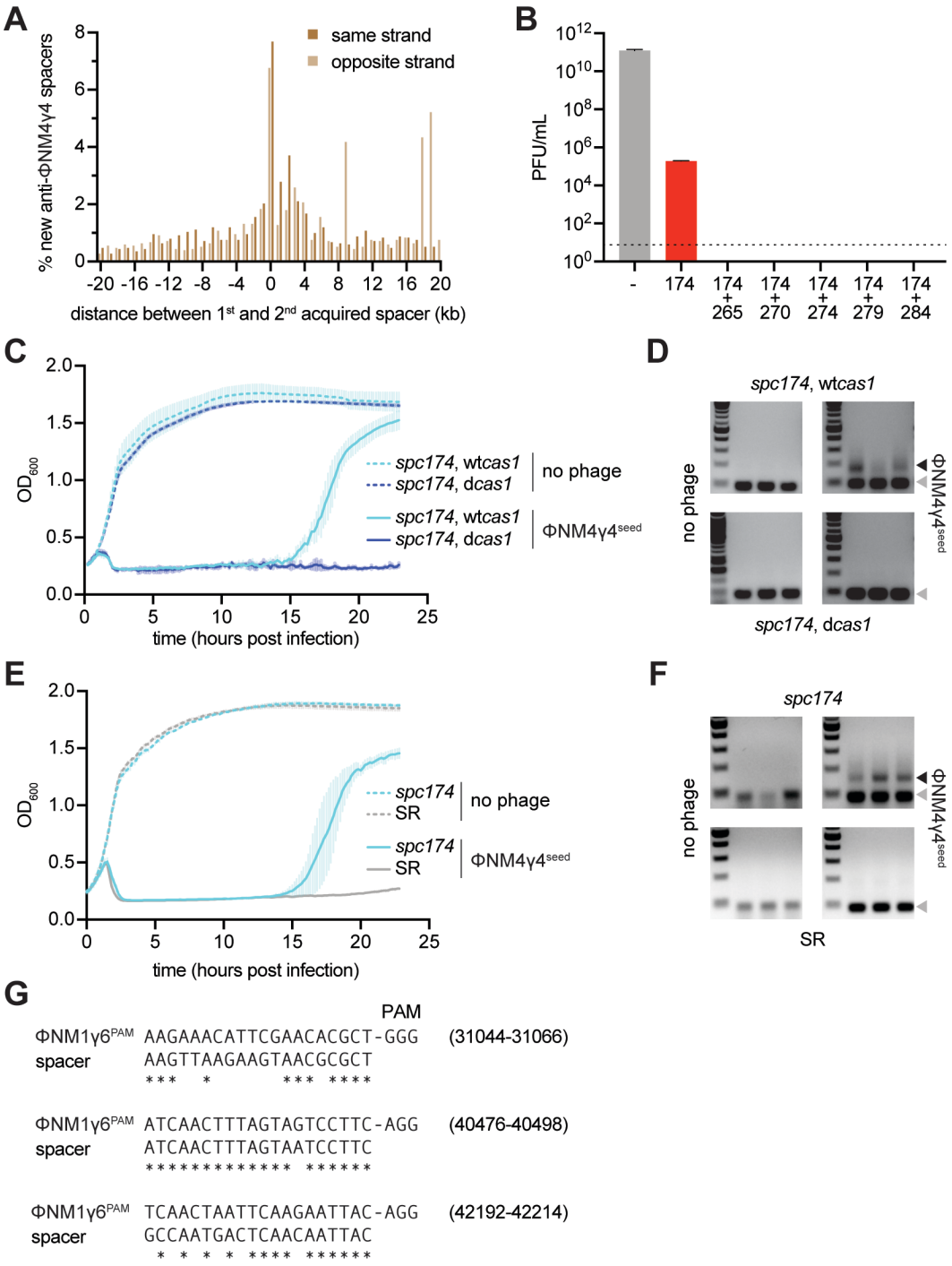

Figure S6. Effects of cleavage-dependent spacer acquisition on the immunity of bacterial cultures. Related to Fig. 6. (**A**) Distance between the targets in the ΦNM4γ4 genome specified by the first and second spacers acquired after infection of naïve staphylococci carrying the type II-A CRISPR-Cas system of *S. pyogenes* with ΦNM4γ4. The number of different spacers within 1-kb bins of the ΦNM4γ4 genome are shown; the position of first spacer acquired in each array is set as 0 kb. Second spacers have been divided into two categories: those targeting the same or the opposite DNA strand as the first acquired spacer. (**B**) Quantification of phage escapers as PFU/ml after the

plating of different dilutions of phage ΦNM4γ4 stock onto plates seeded with different staphylococcal strains that harbor pCRISPR either lacking a targeting spacer (-) or programmed with *spc174* or *spc174* and additional spacer acquired in the experiment of Fig. S3C. Mean ± StDev values of three independent experiments are shown. (**C**) Cell survival measured as OD_{600} after infection of cultures carrying either the wild-type or the nuclease deficient *cas1* gene (wt*cas1* or d*cas1*, respectively) on pCRISPR(*spc174*) with ΦNM4γ4 at MOI 10 or no phage as a control. The average curves of three different replicates are shown, with +/- StDev values shown in lighter colors. (**D**) Agarose gel electrophoresis of PCR products after amplification of the CRISPR array of cells obtained after the experiment in (**C**) to detect the integration of new spacers. Grey and black arrows: non-expanded and expanded, respectively, CRISPR arrays. (**E**) Same as (**C**) but after infection of staphylococci carrying either pCRISPR(SR) or pCRISPR(*spc174*). The average curves of three different replicates are shown, with +/- StDev values shown in lighter colors. (**F**) Same as (**D**) but for the cells obtained after the experiment in (**E**). (**G**) Putative targets of spacers acquired from the ΦNM4γ4 genome ("spacer") on the ΦNM1γ6^{PAM} genome. The PAM and the genomic position of the targets are shown.